

Chemical and Morphological Characterization of Coconut Shell Powder, Epoxy Resin and Coconut Shell Powder/Epoxy Resin Composites

AM Andezai¹, LM Masu¹, M Maringa²

¹Vaal University of Technology, Faculty of Engineering and Technology, Department of Mechanical Engineering, Private Bag X021, Vanderbijlpark, Andries Potgieter Blvd, 1911, South Africa.

²Central University of Technology, Faculty of Engineering and Technology, Department of Mechanical and Mechatronics Engineering, Private Bag X20539, Bloemfontein, 9300, South Africa.

ORCID: 0000-0003-0154-8572 (AM Andezai), 0000-0002-8544-6321 (Prof LM Masu), 0000-0002-8965-1242 (M Maringa)

Abstract

This work focuses on the utilization of coconut shell powder (CSP) as filler in epoxy resin. Coconut, one of the food crops in the world, generates large amounts of waste material namely coconut shell. The physical and chemical properties of CSP were analysed through fourier transform infrared spectra (FTIR), scanning electron microscopy (SEM), thermal gravimetric analysis (TGA), and differential thermal gravimetric analysis (DTA) to develop a better understanding of its properties. Observation under an electron microscope revealed that the coconut shell powder/epoxy resin composites had a high degree of agglomeration, porosity, and that the coconut shell powder was irregularly shaped. fourier transform infrared spectra analysis of CSP revealed fingerprint peaks typical of cellulose and hemicellulose. The results of TGA and DTA analysis showed that pyrolysis of hemicellulose and cellulose was as maximum at 290°C and 315°C, respectively, while the signature for the pyrolysis of lignin could be distinguished.

Keywords: Weight percentage, coconut shell powder, particle, matrix, reinforcement, FTIR, TGA, DTA and SEM

1.0 INTRODUCTION

Generally, coconut shell is used to produce active carbon, mosquito coils and charcoal. Coconut shell is easily processed into powder form called coconut shell powder. The CSP has potential as filler for polymeric materials as it has better properties compared to mineral fillers such as, calcium carbonate, kaolin, mica, and talc of low cost, renewable, minimal health hazard, low density, less abrasion of machinery, biodegradable, and eco-friendly[1-4]. Over the last few years, several researchers have investigated the exploitation of natural fibres as load-bearing constituents in composite materials [5-7]. The use of such materials in composites has increased due to their low cost, recyclability, and competitive strength to weight ratio [8]. Natural fibres consist mainly of cellulose fibrils and hemicellulose embedded in lignin matrix. The cellulose fibrils occur in the form of spirals running all along the length of fibres and render tensile strength to fibres, while lignin provides rigidity to the fibres [9]. The reinforcing efficiency of natural fibres is related to the nature of cellulose

and its crystallinity. The main components of natural fibres are cellulose (40 - 60 wt%), hemicellulose (20 - 40 wt%), lignin (10 - 25 wt%), as well as pectin, and wax trace contents [10,11]. The high content of the hydroxyl group in cellulose is what gives it a hydrophilic character and is the main cause of poor compatibility between cellulose fibres and polymers used as matrices, which leads to the formation of composites with unsatisfactory mechanical properties [12, 13].

Figure 1 shows the structure of cellulose, a polysaccharide, which consist of several thousand units of β -linked D-Glucose linear chains with the basic formulation, $(C_6H_{10}O_5)_n$ [14]. Figure 2 shows the structure of lignin. The basic formulation of lignin varies from one species of plant to another and maybe represented as $(C_{30}H_{36}O_9)_n$ or $(C_{31}H_{34}O_{11})_n$ [15, 16]. Like cellulose, hemicellulose is also a polysaccharide but with shorter sugar chains of 300 - 500 combined basic units, compared to the 7,000-15,000 combined basic units of cellulose. Hemicellulose is branched, unlike cellulose and exists in the form shown in Figure 3[17].

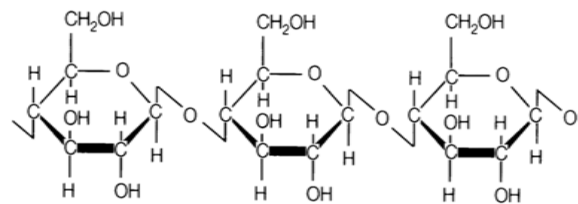


Figure 1: Cellulose structure [14]

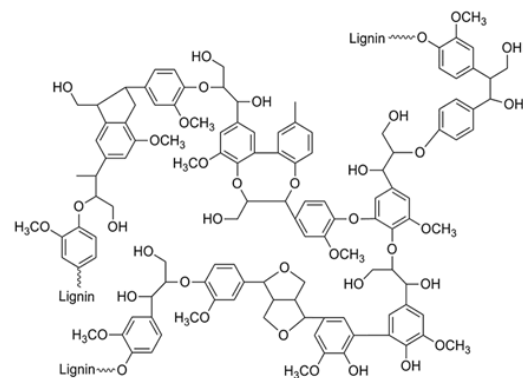


Figure 2: Lignin structure [15, 16]

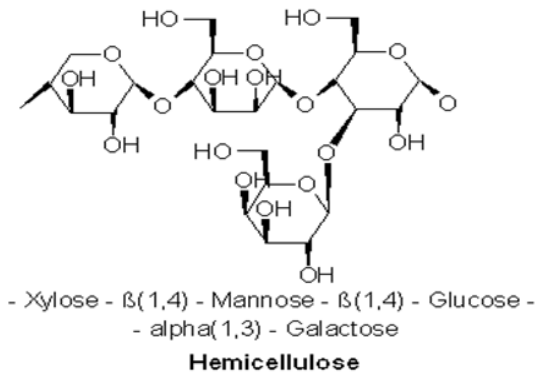


Figure 3: Hemicellulose structure [17]

Coconut fruit from the coco palm tree generates large amounts of waste in the form of coconut shells and efforts to utilise it have resulted mostly in low value or limited applications [14]. The coconut palm (*Cocos nucifera L.*) is one of the most important and useful palms in the world and is an important crop in the agrarian economy of many countries providing food, drink, shelter and raw materials for industries [18]. The coconut palm is undoubtedly the most economically important plant in the palm family and is used as both an ornamental and food crop [18]. The use of the by-products of coconut has been a long-time source of income for many people [18]. The coconut industry in India accounts for over a quarter of the world's total coconut oil output and is set to grow further with the global increase in demand. It is one of the main contributors to the nation's problem of pollution as a solid waste in the form of shells, with an annual production of approximately 3.18 million tonnes [19]. Coconut shells represents more than 60% of India's domestic waste volume. Coconut shells causes problems of disposal, serious enough to constitute an environmental challenge, hence the need to convert them into useful materials to minimize their negative effect on the environment. In developing countries where abundant agricultural waste is generated, the waste can be used as potential industrial raw material or replacement material in the construction and polymer industries. This has the double advantage of reduction in the cost of material in these industries and a means of waste disposal that is more environmentally safe and friendly than other methods of waste disposal commonly in use nowadays [19, 20]. Industrialists in most of the coconut producing countries hail the economic, environmental, and technological benefits of utilizing coconut farm wastes. Worldwide interest in using farm residues for value-added products means that farmers can generate additional income aside from amassing environmental dividends and availing employment opportunities [20]. In this regard, coconut shell powder is an interesting candidate and the use of CSP as a replacement for commercial fillers is thus of great interest [21, 22, 23]. The physical attributes of coconut shell powder are essential in determining their mechanical properties, which in turn predicates the composites physical and mechanical properties [21].

This paper evaluates the physiochemical properties of CSP, epoxy resin and CSP/epoxy resin reinforced composites.

2.0 METHODOLOGY

2.1 Material

Pieces of coconut shells were purchased locally from the market, washed, and dried in sunlight for three weeks to minimise moisture in them and then crushed into smaller pieces using a hammer. The crushed pieces were further ground into powder using a pulveriser machine and ball mills rotating at 6000 rpm shown in Figure 4.



Figure 4: Pulverizing machine and Ball mills machine

The powder was sieved in accordance with BS 1377:1990 standard. Separation of powder was then done using the round vibratory sieve shaker model Endecotts EFL 2000 shown in Figure 5, using different sieving sizes to obtain the required powder sizes for use as fillers of 150 μm and 212 μm under dry conditions.



Figure 5: Round vibratory sieve shaker machine

Figure 6 show the different stages of processing from raw coconut shell powder through to fine sieved powder



Figure 6: Raw coconut shells, crushed coconut shells and coconut shell powder

2.2 Physicochemical Characterization of Coconut Shell Powder

The characterisation of the ground coconut shell powder was conducted at the Vaal University of Technology in the Department of Chemical Engineering, using a Shimadzu FTIR, model 8300 of Kyoto, Japan. FTIR spectra of the powder were recorded in the range of 500-4000 cm^{-1} . The loss of weight of coconut shell particles at different temperatures was studied at the same University with a Japanese, Shimadzu TGA 8000 thermogravimetric analyser. Around 20-30 milligrams of sample was taken and heated up to a final temperature of 900°C and a residence time of 1 minute at 900°C was allowed. TGA was performed at a heating rate of 10°C/Min and 20°C/min. Scanning Electron Microscope micrographs of the coconut shell powder were taken with the help of a Zeiss SEM in the university, as well, to study the morphology of the unused powder, the fractured surfaces of the pure epoxy resin and CSP/epoxy resin composites, and the interfacial interaction between the CSP and epoxy resin in the composite upon application of loads. The epoxy and CSP/epoxy resin composite samples for examination were obtained by cutting sections of about 5 mm in length from the fractured zone. The fractured surfaces of the samples were dusted with gold, placed into a SEM, and analysed.

3.0 RESULTS AND DISCUSSION

The results of thermo-gravimetric analysis, fourier transform infrared spectra, and SEM of CSP, epoxy and CSP/epoxy resin composites with different weight percentages of the CSP filler for the two different CSP filler mean diameters are presented in Figures 7-10, together with their accompanying discussions.

3.1 Thermo-Gravimetric and Differential Thermogravimetric Analysis of CSP

Figure 7 shows the TGA and the DTA Analyse curves of coconut shell powder

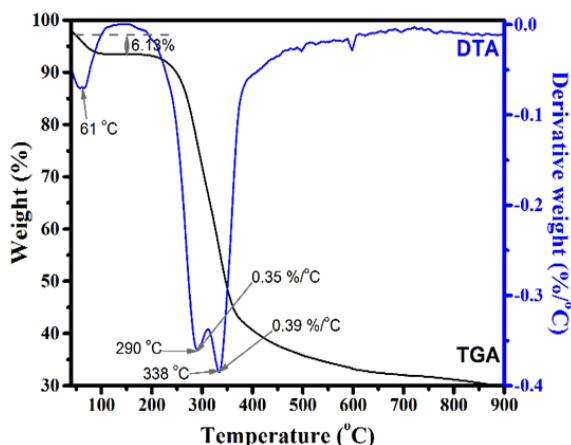


Figure 7: Thermogravimetric and Differential Thermogravimetric curves of CSP

The first peak of the DTA curve of CSP in Figure 7 with a corresponding mass loss of 6.13% as read from the TGA curve refers to the loss of moisture between 0°C and 100°C. After the initial loss of the moisture, the remaining material in CSP remained thermally stable up to a temperature of 200°C on the

TGA curve. After that, the rate of pyrolysis increased until it reached a maximum rate of about 0.35 mass % per °C at 290°C. After a brief reduction of the rate of pyrolysis from a temperature of 290°C - 315°C, it increased again to a maximum rate of about 0.39 mass % per °C at a temperature of 338°C. A sudden drastic drop in pyrolysis was observed beyond this point. From 400°C - 900°C, pyrolysis continued progressively at a low rate, thus resulting in tailing-off of the TGA curve. The first peak in the DTA curve at 290°C is attributed to pyrolysis of hemicellulose, and the second peak starting from 315°C and the long tail due to the pyrolysis of cellulose and lignin, respectively [11, 21]. Therefore, the rate of pyrolysis is maximum for hemicellulose, and cellulose at temperatures of 290°C, and 338°C, respectively, which is consistent with the work of Liyange et al. [21]. It is important to note that despite CSP having three main material constituents of cellulose, hemicellulose and lignin, only two peaks, one each for the first two constituents, were observed in the DTA curve of CSP. That the peak for lignin is not prominent is consistent with the known gradual pyrolysis of the component between room temperature and 900°C [11].

Due to the high decomposition rate per unit time, the rapid decomposition zone or second stage of decomposition of cellulose is treated as an active pyrolytic zone. During this stage, the intermolecular associations and weaker chemical bonds are destroyed. Yang et al. [24] stated that 93.5% of pure cellulose was pyrolysed between temperatures of 315°C - 400°C.

Previous work by Singh et al. [25] clearly shows the amount of CSP pyrolysed within the temperature range 315°C - 400°C to be about 30% by mass. Pyrolysis was observed in this work to decompose the main constituents of CSP in the temperature ranges, hemicellulose 200 - 260°C, cellulose 240 - 350°C, and lignin 300°C - 500°C. In the present work, however, hemicellulose started decomposing at 290°C and cellulose at 338°C. The removal of moisture early in the process is assisted by the exothermic pyrolysis of lignin and cellulose [11] as is evidenced by the upturn of the DTA curve between temperatures of 61 - 100°C. The pyrolysis of lignin is known to occur slowly between room temperature and 900°C [11]

The curves in Figure 7 demonstrate significant differences in the pyrolysis behaviour of the three main components of CSP. Hemicellulose was the first to decompose significantly in the temperature range 290-315°C. This was followed by decomposition of cellulose in the temperature range 315-338°C, while the decomposition of lignin does not feature in the figure for the reasons stated above but is known from published research to occur from room temperature to 900°C. At low temperatures (<400°C) the pyrolysis of hemicellulose and lignin are exothermic reactions, while that of cellulose is endothermic. However, at high temperatures (>400°C), the situation reverses and the pyrolysis of the first two becomes endothermic while that of the cellulose becomes exothermic, a distinction that is not clear from the DTA curve in Figure 7 but was shown to be the case in the work of Yang et al. 2007 [11]. The results of this work coincide well with those of Yang et al. [24] that showed the maximum pyrolysis rate of hemicellulose to start at a temperature of 315°C and that of cellulose is at 338°C.

3.2 Fourier Transform Infrared Spectra of CSP

Figure 8 shows the FTIR spectra of coconut shell powder

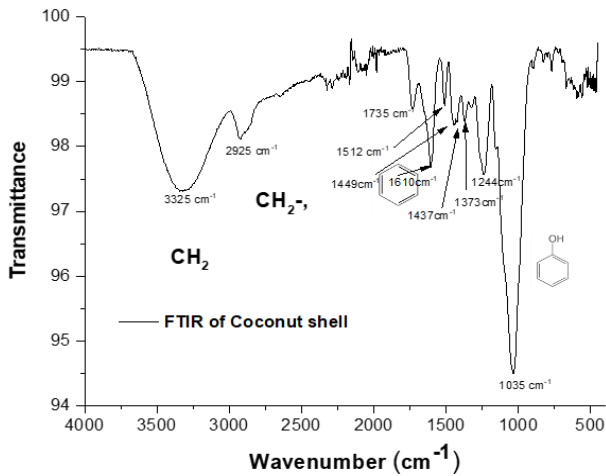


Figure 8: FTIR spectra of coconut shell powder

The FTIR spectrum shown in Figure 8 provides information on the chemical composition of coconut shell powder. Interpretation of this spectra is based on the works of Yang et al. [11] and Liyange et al. [21]. Stretching of the hydroxyl group (OH) bond was seen as a broad peak in coconut shell powder around a wavelength of 3325 cm⁻¹ due to the hydrogen

bonding in the cellulose. The peak at 2925 cm⁻¹ was due to the stretching vibration of the C-H bond. Absorption at 1735 cm⁻¹ was due to stretching of the carboxyl bond C=O of the acetyl group in hemicellulose. The peak at 1512 cm⁻¹ contributed to the conjugated C-O group for the aromatic skeletal in lignin, and peak at 1449 cm⁻¹ referred to C-H group of lignin. The prominent peak at 1610 cm⁻¹ in the spectrum is due to stretching-vibration of the C=C bond in the benzene ring. Absorbance in the region of 1512 cm⁻¹ observed in lignin is probably due to vibrations in the aromatic ring, while the peaks around 1449 cm⁻¹ are due to stretching- vibration of the O-CH₃ bonds that are found in lignin. The peak at 1244 cm⁻¹ is probably due to stretching-vibration of the C-O bond in the C-OH phenolic group [11, 21, 26].

3.3 Scanning Electron Microscopy of, CSP, Epoxy Resin and CSP/Epoxy Resin Composites

In this section is presented SEM micrographs of CSP powder, epoxy resin and CSP/epoxy resin composites that were used to study the morphology of the CSP powder and microstructure of the matrix and composites.

3.3.1 The Morphology of CSP

Figure 9(a), (b) and (c) shows the SEM micrographs of crushed coconut particles at different magnifications of 10,000x, 10,050x and 20,000x.

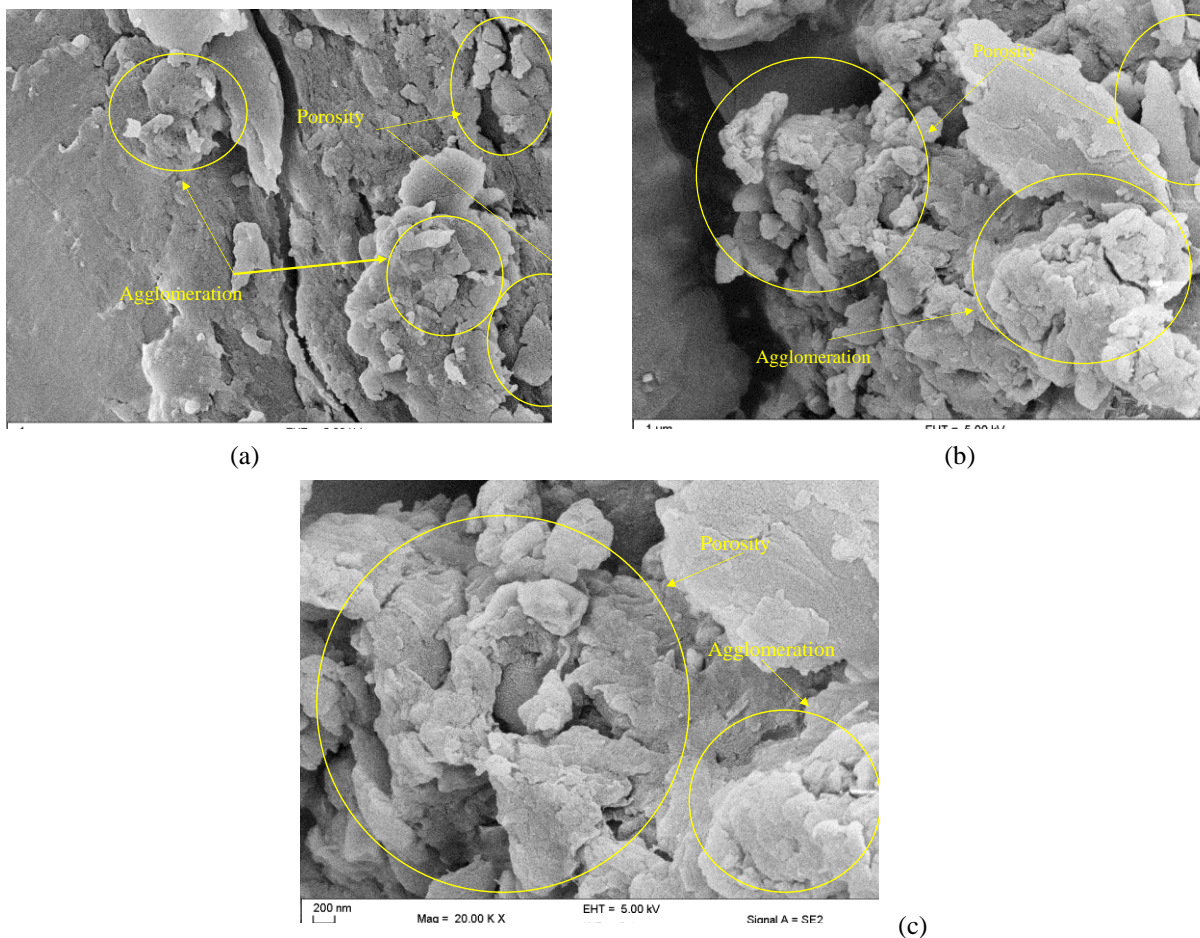
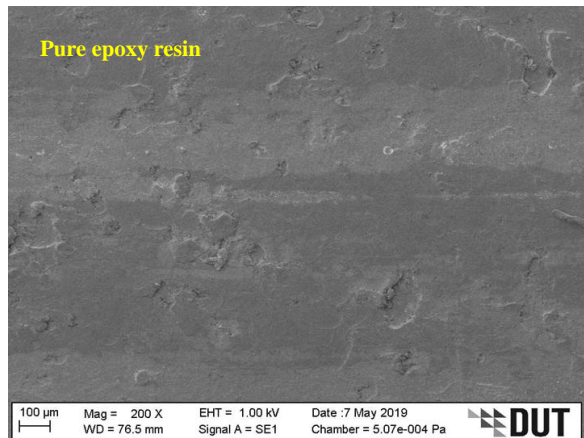


Figure 9: Particle SEM image of coconut shell powder under 10,000x 10,050x and 20,000x magnifications

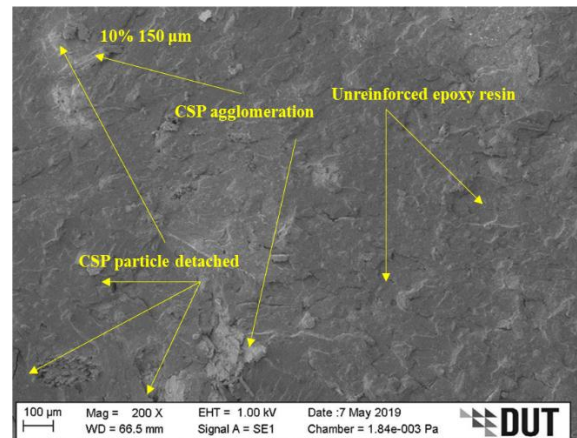
The SEM micrographs shown in Figure 9 revealed CSP particles that were angular and irregular in shape. The raw CSP in seen in these micrographs to be highly porous, agglomerated and irregularly shaped. It was not possible to detect a single stand-alone particle even at higher magnifications using SEM, which a sign of the degree of agglomeration of the CSP particles. Clearly the raw CSP particles require to be sieved in order to obtain particles of known sizes that can be used as filler for reinforcement.

3.3.2 The Microstructures of pure epoxy resin and reinforced CSP/epoxy resin composites

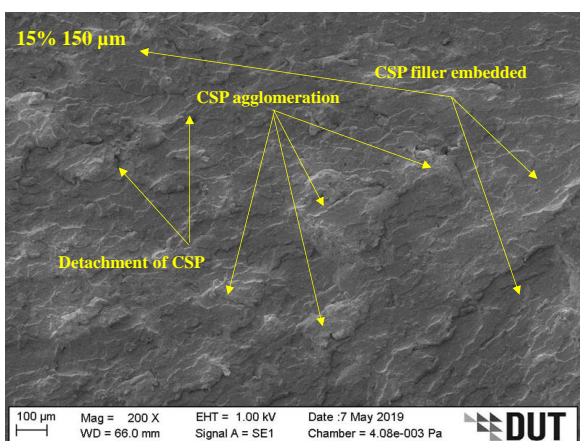
Figure 10(a) shows a SEM micrograph of pure epoxy resin, while Figure 10(b), (c), (d), (e), (f) and (g) show SEM micrograph of CSP/epoxy resin composites of the different weight fractions of 10% , 15% and 20% for the 150 μm and 212 μm CSP particle sizes.



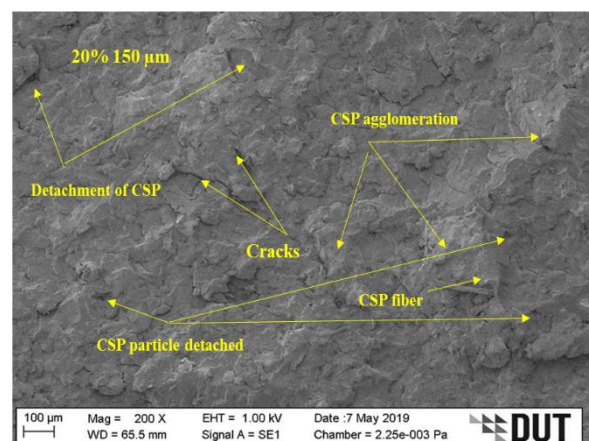
(a)



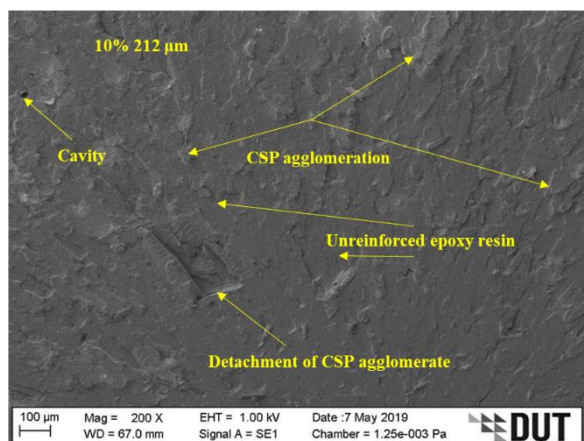
(b)



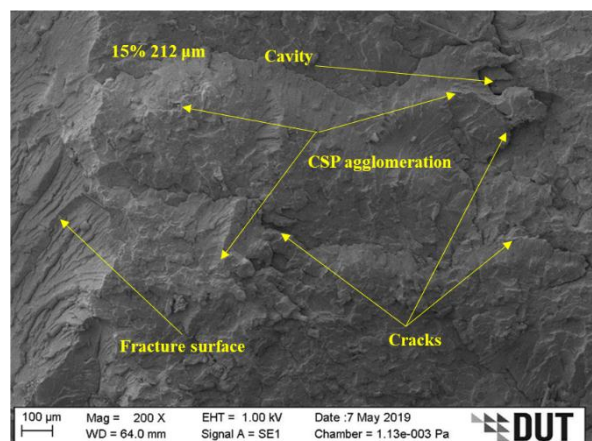
(c)



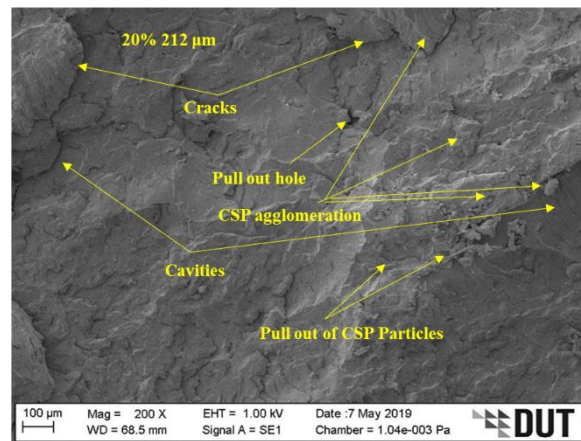
(d)



(e)



(f)



(g)

Figure 10: SEM micrographs of the neat epoxy resin and reinforced CSP/epoxy resin composites for different weight fractions of 10%, 15% and 20% of the 150 μm and 212 μm CSP particle sizes

In the SEM micrographs in the preceding figure, cases of pull out and detachment of CSP particles are observed. Tear cavities are also noted and are thought to be centers around which eventual fracture and separation of the specimens occurred. It is observed in these micrographs that CSP was embedded in the resin, mainly as agglomerates, and that some cavities existed from pulled-out CSPs particles. Irregular cracks of varying lengths longer and shorter than the size of the reinforcing fillers were observed in Figure 10d, f and g. The failure surfaces in these three micrographs are very irregular, suggesting that the lines of fracture were defined by the presence of the filler particles. This is consistent with theory that shows fillers to act as crack arrestors. In addition, Figures 10b, c and e show signs of smooth fracture surfaces consistent with the failure of pure epoxy resin. This indicates that the filler volume fraction was not adequate to spread throughout the epoxy resin at these low filler volume fractions. The presence of large cavities in some of the micrographs is evidence of interfacial bond failure between the CSP agglomerates and the epoxy resin matrix. The large cavities show aligned patterns that are inclined and are a sign of shear failure as the agglomerates are separated from the matrix. It is evident from the micrographs that with increasing weight percentage of the CSP particles, agglomeration of CSP particles increases. For most of the mechanical properties reported in a previous publication, the CSP/epoxy resin composites of the 150 μm particles showed better properties than the 212 μm particles [27, 28]. The ties in with the higher levels of agglomeration and higher incidences of large cavities in the composites of the larger particles. Similar phenomena were observed elsewhere for groundnut shell particles reinforced epoxy composites [29], periwinkle shell particles reinforced polyester composites [30] and for coconut shell reinforced polymer matrix composites [31].

4.0 CONCLUSION

The following conclusions can be drawn from this work:

- 1) From the SEM micrographs analysis, it was clearly observed that interaction between the coconut shell particles and the matrix decreased with increase in the

coconut shell particles content which caused poor bonding and considered to be a major factor responsible for the decrease in strength when compared with the pure epoxy resin having no coconut shell particles observed elsewhere, as noted in the previous paragraph.

- 2) The morphology of the CSP/epoxy resin composites showed high degree of agglomeration and irregular cracks of varying lengths different from the size of the reinforcing filler particles.
- 3) FTIR analysis of CSP showed fingerprint peaks which are synonymous to cellulose and hemicellulose.
- 4) The TGA and DTA analysis showed that pyrolysis of hemicellulose and cellulose was a maximum at 290°C and 315°C, while the signature for the pyrolysis of lignin could not be differentiated.

5.0 CONFLICT OF INTEREST

The researchers have no conflict of interest to disclose with regard to the current research work.

ACKNOWLEDGEMENT

This research work was supported by the Vaal University of Technology (VUT), South Africa and Council for Scientific and Industrial Research (CSIR), South Africa.

REFERENCES

- [1] Perinovic, S., Andricic, B., Erceg, M., 2010, "Thermal properties of poly (L -lactic)/olive stone flour composites". *Thermo. chim. Acta*, Vol. 510, pp. 97-102.
- [2] John, M.J., and Anandjiwala, R.D., 2009, "Chemical modification of flax reinforced polypropylene composites". *Compos. A*, Vol. 40, pp. 442-448.
- [3] Zaman, H.U., Khan, M.A., Khan, R.A., and Beg, Md.D.H., 2011, "A comparative study on the mechanical, degradation and interfacial properties of

- jute/LLDPE and jute/natural rubber composites". *Int. J. Polym. Mater.* Vol. 60, pp. 303-315.
- [4] Tserki, S., Matzinos, P., Kokkou, S., and Panayiotou, C., 2005, "Novel biodegradable composite based on treated lignocellulosic waste flour as filler" *Part I. Surface chemical modification and characterization of waste flour. Compos. A*, Vol. 36, pp. 965-974.
- [5] Eicorn, S.J., 2001, "Review Current International Research into Cellulosic Fibers and Composites". *Journal of Material Science*, 36, pp.2107-2131.
- [6] Sarasini, F., and Fiore, V., 2018, "A systematic literature review on less common natural fibres and their biocomposites". *Journal of cleaner production*, 195, pp.240-267.
- [7] Salit, M.S., 2014, "Tropical natural fibre composites". *Tropical Natural fibers and their properties*, p.15.
- [8] Das, S., 2001, "*The cost of automotive polymer composites: a review and assessment of DOE's lightweight materials composites research* (p. 47). Oak Ridge, Tennessee, USA: Oak Ridge National Laboratory.
- [9] John, M.J. and Anandjiwala, R.D., 2008, "Recent developments in chemical modification and characterization of natural fiber- reinforced composites". *Polymer composites*, 29(2), pp.187-207.
- [10] Hasanah, U., Setiaji, B., Triyono and Chairil Anwar, C., 2012, "The Chemical Composition and Physical Properties of the Light and Heavy Tar Resulted from Coconut Shell Pyrolysis". *J. Pure App. Chem. Res.*, 1(1), pp. 26- 32.
- [11] Yang, H., Yan, R., Chen, H., Lee, D.H. and Zheng, C., 2007, "Characteristics of hemicellulose, cellulose and lignin pyrolysis". *Fuel*, 86(12-13), pp.1781-1788.
- [12] Saheb, N.D., and Jog J.P., 1999, "Natural fibre polymer composites": a review. *Adv Polym Technol*; Vol. 18, pp. 351-363. 21.
- [13] Glasser Wg, Et Al., 1999, "Fibre-reinforced cellulosic thermoplastic composites". *J Appl Polym Sci*; Vol. 73, pp. 1329-1340.
- [14] Festucci-Buselli, R.A., Otoni, W.C. and Joshi, C.P., 2007, "Structure, organization, and functions of cellulose synthase complexes in higher plants". *Brazilian Journal of Plant Physiology*, 19(1), pp.1-13.
- [15] Martone, P.T., Estevez, J.M., Lu, F., Ruel, K., Denny, M.W., Somerville, C. and Ralph, J., 2009, "Discovery of lignin in seaweed reveals convergent evolution of cell-wall architecture". *Current biology*, 19(2), pp.169-175.
- [16] Lu, Y., Lu, Y.C., Hu, H.Q., Xie, F.J., Wei, X.Y. and Fan, X., 2017, "Structural characterization of lignin and its degradation products with spectroscopic methods". *Journal of Spectroscopy*, 2017.
- [17] Ebringerová, A., 2005, December. Structural diversity and application potential of hemicelluloses. In *Macromolecular symposia* (Vol. 232, No. 1, pp. 1-12). Weinheim: WILEY- VCH Verlag.
- [18] Uwubanmwen, I.O., Nwawe, C.N., Okere, R.A., Dada, M. and Eseigbe, E., 2011, "Harnessing the potentials of the coconut palm in the Nigerian economy". *World journal of agricultural sciences*, 7(6), pp.684-691.
- [19] Kaur, M. and Kaur, M., 2012, "A review on utilization of coconut shell as coarse aggregate in mass concrete". *International journal of applied engineering research*, 7(11), pp.05-08.
- [20] Ganiron Jr, T.U., 2013, "Sustainable Management of Waste Coconut Shells as Aggregates in Concrete Mixture". *Journal of Engineering Science & Technology Review*, 6(5).
- [21] Liyanage, C.D., and Pieris, M., 2015, "A physic-chemical analysis of coconut shell powder", *Procedia Chemistry*, Vol. 16, pp. 222-228.
- [22] Azlina, W., Ghani, W.A.K., Mohd Syafik Firdaus, A., Amin, K., Azil Bahari, A. and da Silva, G., 2010, "Physical and thermochemical characterisation of Malaysian biomass ashes".
- [23] Sareena, C., Ramesan, M.T. and Purushothaman, E., 2012, "Utilization of coconut shell powder as a novel filler in natural rubber". *Journal of Reinforced Plastics and Composites*, 31(8), pp.533-547.
- [24] Yang, H. S., Kim, H.J. Lee, B.J., and Hawng, T.S., 2004, "Rice husk flour filled polypropylene composites, mechanical and morphological study". *Composite Structure*. Vol. 63, pp. 305-315.
- [25] Singh, S., Finner, M., Rohatgi, P., Buelow, F., and Schaller, M., 1991, "Structure and mechanical properties of corn kernels: a hybrid composite material". *Journal of Material Science*, 26(1), pp. 274-284.
- [26] Chun, K.S., Husseinsyah, S. and Osman, H., 2013, "Properties of coconut shell powder- filled polylactic acid ecocomposites": Effect of maleic acid. *Polymer Engineering & Science*, 53(5), pp.1109-1116.
- [27] Andezai, A.M., Masu, L.M., and Maringa, M., 2020, "Experimental investigation of dynamic elastic properties of reinforced coconut shell powder/epoxy resin composites". *International Journal of Engineering Research and Technology*, 13(10), pp. 2765-2772.
- [28] Andezai, A.M., Masu, L.M., and Maringa, M., 2020, "Investigating the mechanical properties of reinforced coconut shell powder/epoxy resin composites". *International Journal of Engineering Research and Technology*, 13(10), pp. 2784-2793
- [29] Raju, G.U., and Kumarappa, S., 2011, "Experimental study on mechanical properties of groundnut shell particle reinforced epoxy composites". *Journal of Reinforced Plastics and Composites*, Vol.30, pp. 1029-1037.
- [30] Njoku, R.E., Okon, A.E., and Ikpaki, T.C., 2011, "Effects of variation of particle size and weight fraction on the tensile strength and modulus of periwinkle shell reinforced polyester composite", *Nigerian J. Technol.* Vol. 30, pp. 87-93.
- [31] Agunsoye, J.O., Isaac, T.S. and Samuel, S.O., 2012, "Study of mechanical behaviour of coconut shell reinforced polymer matrix composite". *Journal of minerals and materials characterization and Engineering*, 11(8), pp.774-779.